

Phase transitions in soft matter systems

H. Löwen*, M. Watzlawek*, C. N. Likos*, M. Schmidt*, A. Jusufi*,
H. Graf*, A. R. Denton[◇], C. von Ferber*

* Institut für Theoretische Physik II, Heinrich-Heine-Universität Düsseldorf, Universitätsstraße 1,
D-40225 Düsseldorf, Germany

[◇] Department of Physics, Acadia University, Wolfville, Nova Scotia, Canada B0P 1X0

Abstract. We review recent work on fluid-solid and solid-solid phase transitions in soft matter systems such as colloidal suspensions and star polymer solutions. Starting from a given interparticle pair potential we predict the corresponding phase diagrams using computer simulations, cell theory, and density functional theory. When possible, the results are compared with experimental data. In particular, we discuss the following aspects: a cascade of freezing transitions for confined colloids, stable one-component quasicrystals for charged colloids, reentrant melting and anisotropic solid phases for star polymer solutions and reentrant nematic ordering for suspensions of the tobacco-mosaic virus.

PACS: 64.70.-p, 82.70.Dd, 61.25.Hq

I. INTRODUCTION

One of the major challenges in statistical physics is to understand and predict the macroscopic phase behaviour for different temperatures and densities from a microscopic many-body theory provided the interaction between the particles is known (1, 2). Typically this interaction is specified in terms of a radially symmetric pair potential $V(r)$ where r is the particle separation. Important progress was made during the last decades in predicting the thermodynamically stable phases for simple inter-molecular pair potentials, such as Lennard-Jones-systems, plasmas or hard spheres, using computer simulations (1) and classical density functional theory of freezing (3). An important realization of classical many-body systems are suspensions of mesoscopic-sized colloidal particles dispersed in a fluid medium. Colloidal samples have quite a number of advantages over molecular ones: First, their effective pair interaction $V(r)$ is eminently tunable through experimental control of particle and solvent properties (4). This brings about more extreme pair interactions than the molecular ones leading to novel phase transformations. Second, colloidal suspensions can be studied in real space by, e.g., video-microscopy

which leads to direct experimental observations. Third, colloids can be confined in a well-controlled way which gives rise to new fascinating phenomena.

If the colloidal particles are sterically stabilized against coagulation, the “softness” of the interparticle repulsion is governed by the length of the polymer chains grafted onto the colloidal surface and their surface grafting density. Computer simulations (5) and theory (6) have revealed that a fluid freezes into a body-centred-cubic (*bcc*) crystal for soft repulsions and into a face-centred-cubic (*fcc*) crystal for strong repulsions. This was confirmed in experiments on sterically-stabilized colloidal particles (7). A similar behaviour occurs for charge-stabilized suspensions where the “softness” of $V(r)$ is now controlled by the concentration of added salt (8). Less common effects were observed for potentials involving an attractive part aside from a repulsive core as induced, e.g., by added non-adsorbing polymer coils. In reducing the range of the attraction, a vanishing liquid phase could be observed (9) and an isostructural solid-solid transition was predicted for an extremely short-ranged attraction (10).

In the present paper we review recent work concerning unexpected phase behaviour for peculiar pair potentials which are realized for colloidal suspensions and star polymer solutions. We first discuss sterically-stabilized colloids between two parallel glass plates modelled by hard spheres confined between two hard walls. A rich phase diagram including different layering transitions is obtained. Then we investigate the phase behaviour of a very soft potential diverging logarithmically with distance r at the origin. This potential is realized for star polymers in the scaling regime. We then exploit the full tunability of colloidal interactions in order to predict stable one-component quasicrystals for interactions which possess both attractive and repulsive parts as realized for index-matched charged suspensions with added non-adsorbing polymers. Finally we show that the phase diagram of the rod-like tobacco-mosaic-virus exhibits different liquid crystalline phases with a re-entrant nematic transition. The theoretical tools used to calculate the phase behaviour are computer simulations, density functional theory, liquid integral equations and solid cell models.

II. FREEZING IN CONFINING GEOMETRY

The model we discuss here consists of hard spheres of diameter σ confined between two parallel plates of distance H . The thermostistical properties in equilibrium depend solely on two parameters, namely the reduced density $\rho_H = N\sigma^3/(AH)$ (where N is the number of spheres and A the system area) and the reduced plate distance $h = H/\sigma - 1$. Clearly one can continuously interpolate between two and three spatial dimensions by tuning the plate distance: For $H = \sigma$, our model reduces to that of two-dimensional hard discs while for $H \rightarrow \infty$ the three-dimensional bulk case is recovered.

The equilibrium phase diagram as obtained by Monte-Carlo computer simulation in the $\rho_H - h$ -plane (11, 12) is shown in Fig. 1 for moderate plate distances h . The phase behaviour is very rich and much more complicated than in the bulk. Cascades of different

solid-solid transitions are found. For low densities the stable phase is an inhomogeneous fluid. All possible stable solid phases are also realized as close-packed configurations (13, 14) for a certain plate distance. Accordingly one finds stable layered structures involving intersecting triangular lattices (1Δ , 2Δ) and intersecting square lattices ($2\Box$). Also a buckled phase (b) and a phase with a rhombic elementary cell (rhombic phase (r)) are stable. All transitions are first-order.

Similar phases were found in experiments of highly salted charged colloids between glass plates (15–17). Here even higher reduced plate distances were studied. There is compelling evidence that a prism-phase consisting of alternating prisms built up by spheres is the close-packed configuration in certain domains of h (17). Still a full quantitative mapping of the experimental data onto the theoretical phase diagram of Fig. 1 has to be performed.

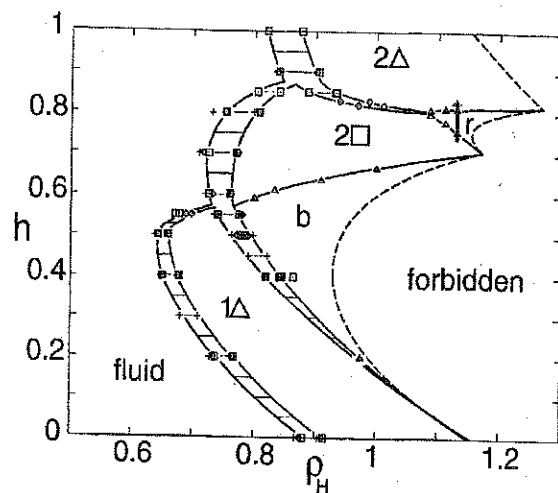


FIGURE 1: Phase diagram for hard spheres of reduced density ρ_H between parallel plates with effective reduced distance h . Symbols indicate different system sizes: $N = 192$ (+); $N = 384, 512$ (\diamond); $N = 576$ (Δ); $N = 1024, 1156$ (\square). Six phases occur (fluid, 1Δ , b , $2\Box$, r and 2Δ). The closed-packed density is marked by a dashed line. Solid lines are guides to the eye. Thin horizontal lines represent two-phase coexistence. From Refs. (11, 12).

Let us comment on further related aspects of the model: First it would be nice to perform a full theoretical calculation for the phase diagram of hard spheres between hard plates. It was already shown that a solid cell theory combined with a simple fluid state free energy gives the same topology of the phase behaviour (11, 12). It would be inter-

esting to do a density functional calculation e.g. with Rosenfeld's functional which possesses the correct geometry excluding configurations of overlapping spheres (18). Second, one should investigate different confining shapes. Intriguing examples are circular and polyhedral boundaries in two dimensions. Studies have been made for confined hard discs (19) and for magnetic colloids in several geometries (20). Third, similar layering transitions occur for charged systems, such as confined electrons (21) or plasma sheets (22). We also note that one should investigate in more detail the stability of phases with long-range orientational order decaying algebraically for large distances. Apart from the well-known hexatic phase also conceivable are "tetratic" or "duatic" phases, where four-fold and twofold symmetry, respectively, persists over large distances. Finally there is a mathematical proof for the close packed structure for small h , $h \leq \sqrt{2}/2$ (23) comprising the 1Δ , b and $2\Box$ phase. A proof for higher h is still lacking, however. Related recent work has focused on a rigorous proof in the three-dimensional bulk (24) or for different confinements (25).

III. PHASE TRANSITIONS IN STAR POLYMER SOLUTIONS

A star polymer consists of f linear polymer chains that are attached to a common microscopic core (26). The typical extension of such a star in a good solvent is governed by the so-called corona diameter σ , which measures the spatial extension of the monomer density around a single star. In a concentrated solution with a finite star number density ρ , the stars are interacting. The interaction is repulsive due to the restriction of allowed configurations for the polymer chains from different centers. In a first approximation, the interaction is pairwise. An explicit form for the pair potential $V(r)$ was proposed recently: it consists of an ultrasoft part inside the coronae and falls off exponentially with core-core distance r outside the coronae of two stars. In detail,

$$V(r) = \begin{cases} \frac{5}{18} k_B T f^{3/2} \left[-\ln\left(\frac{r}{\sigma}\right) + \frac{1}{1+\sqrt{f/2}} \right] & \text{for } r \leq \sigma \\ \frac{5}{18} k_B T f^{3/2} \frac{\sigma}{1+\sqrt{f/2}} \frac{\exp(-\sqrt{f}(r-\sigma)/2\sigma)}{r} & \text{for } r > \sigma \end{cases} \quad (1)$$

Here $k_B T$ is the thermal energy and f is the arm number of a single star. As the effective interaction is purely entropic, it simply scales with the thermal energy. There are many facts confirming that this pair potential [Equation (1)] provides for a reasonable description of the effective interaction between the stars: (i) The behaviour for very small r ($r \ll \sigma$) is consistent with scaling theory (27, 28). (ii) Microscopic Molecular Dynamics computer simulations have been performed for several values of f and different monomer numbers per chains (29). They reproduce perfectly the overall shape of the effective interaction. (iii) The scattering intensity for small-angle neutron scattering data could be well-described by this pair potential without any fitting parameter for an 18-arm star (28, 30).

Based on Monte-Carlo computer simulations for the pair potential (1), the phase diagram of star polymer solutions was calculated recently (31). In the plane spanned by the reduced density $\eta = \pi\rho\sigma^{3/6}$ and the inverse arm number $1/f$ the results are displayed in Fig. 2.

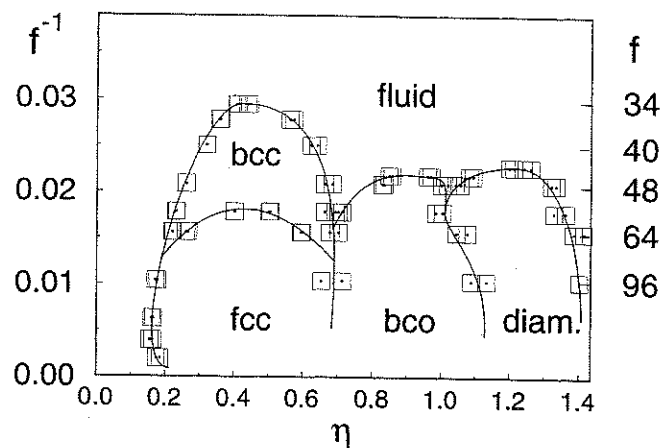


FIGURE 2: The phase diagram of star polymer solutions for different arm numbers f versus reduced density η . The squares are the results from computer simulation and mark coexistence conditions. The lines are a guide to the eye.

Remarkably, there is no freezing below a critical arm number $f_c \approx 34$. For $f > f_c$ there is freezing, with increasing density, into a *bcc* lattice, which then remelts upon further compression. This is in accordance with an earlier qualitative analysis of Witten et al. (32) For higher arm numbers, freezing into an *fcc* lattice occurs, since the potential is becoming steeper as f is increasing. For higher densities, however, there are less common solid structures: an anisotropic body-centered orthorhombic phase as well as a diamond lattice become stable. This is the first time that such crystal structures have been determined to be stable for radial symmetric pair potentials. Obviously this is due to the ultrasoft core together with the crossover at distances comparable to the corona diameter of the stars (31). A very peculiar behaviour occurs for intermediate arm number $f \approx 48$: Increasing the density, the system first freezes, then remelts, then refreezes. Such behaviour also has been found experimentally in spherical diblock copolymer micelles by Gast and coworkers (33).

Apart from the full experimental verification of the phase diagram, there is still the theoretical question about the relevance of triplet and other many-body interactions for higher densities. Recent calculations, based on scaling theory and computer simulation, have shown, however, that the triplet contributions are only 11% of the pairwise inter-

action (34). We finally remark that the interaction depends sensitively on the solvent quality and on the nature of polymer chains adsorbed onto the core. For a poor solvent close to the so-called Θ conditions the potential has a completely different form (35). If a polyelectrolyte such as gelatin is adsorbed instead of a neutral chain, again the effective interaction changes completely (36).

IV. COLLOIDAL QUASICRYSTALS

We now consider a perhaps more "exotic" interaction which is, however, actually realized in colloidal suspensions. Colloidal particles that are charged, sterically stabilized by adsorbed polymer brushes, and mixed in solution with non-adsorbing polymer coils exhibit an effective interaction that can be widely varied via the particle charge and the osmotic pressure of the added polymer coils. The total potential $V(r) = V_1(r) + V_2(r) + V_3(r)$ consists of three parts: $V_1(r)$ is a hard-sphere potential which forbids overlaps of two spheres of diameter σ . The colloidal charge results in an effective screened Coulomb repulsion

$$V_2(r) = \frac{Z^2 e^2}{\epsilon} \left[\frac{\exp(\kappa\sigma/2)}{1 + \kappa\sigma/2} \right]^2 \frac{\exp(-\kappa r)}{r} \quad (2)$$

Here, e is the elementary charge, Z is the total colloidal charge number, ϵ is the dielectric constant of the solvent, and the inverse Debye-Hückel screening length κ is defined as $\kappa = \sqrt{4\pi e^2 Z \rho / \epsilon k_B T (1 - \eta)}$. Finally the added polymer gives rise to a depletion attraction which can be modelled by the Asakura-Oosawa expression (37)

$$V_3(r) = -c \left[1 - \frac{3x}{2(1+\xi)} + \frac{1}{2} \left(\frac{x}{1+\xi} \right)^3 \right] \quad (3)$$

where $x = r/\sigma$, $\xi = 2R_g/\sigma$ where R_g is the radius of gyration of the polymer coils, and $c = (\pi/6)\Pi_p\sigma^3(1+\xi)^3$. The physical meaning of Π_p is the osmotic pressure of the added polymer which can be controlled and varied by the polymer concentration. For appropriate parameters, the total potential $V(r)$ has a repulsive hard core, then becomes attractive as r grows, and finally changes to repulsive at longer range. Hence the stability of solid phases depends sensitively on the range of the attraction. At a given colloidal number density ρ , a solid structure is energetically favourable if the nearest neighbours experience the minimum in the potential.

A detailed survey of possible solid structures has been performed in Ref. (38). A density-functional-perturbation study has revealed that for an attraction of range roughly 10–30% of σ and depth a few a few $k_B T$ units a quasicrystalline structure can be stabilized. This result was obtained by comparing the free energies of a rational approximant model of an icosahedral quasicrystal to those of the common crystalline structures. A

phase diagram is shown in Fig. 3, which illustrates that above a threshold polymer pressure the liquid-solid transition is characterized by first-order freezing into a quasicrystalline structure. It has to be emphasized that this is a one-component quasicrystalline lattice of colloidal spheres. This has never been seen to be stable in atomic systems but may be realized for colloidal suspensions. The relevant range of polymer pressures Π_p is high but not completely beyond experimental realization. A computer simulation that would test the prediction of the approximate theory and ultimate experimental verification of this fascinating phase still lie ahead.

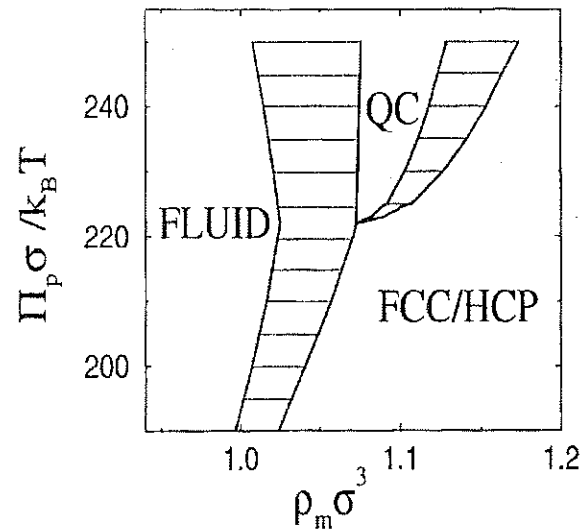


FIGURE 3: Phase diagram of polymer osmotic pressure versus reduced macroion density $\rho\sigma^3$ for a colloid-polymer mixture interacting via pair potential $V(r)$ as given in section IV. Horizontal tie lines connect corresponding points on coexistence curves. The parameters are: $\sigma = 50$ nm, $Z = 150$, $R_g/\sigma = 0.125$, $T = 297$ K, $\epsilon = 78$. From Ref. (38).

V. TOBACCO MOSAIC VIRUS (TMV) SUSPENSIONS

The tobacco mosaic virus (TMV) is a rigid rod-like particle with a length $\ell_{TMV} = 300$ nm and a diameter of 18 nm. In aqueous solution, concentrated suspensions of TMV particles interact via a repulsive screened electrostatic interaction since they are charged

particles. A suitable description of these interactions which was proved by "ab initio" computer simulations (39) is a Yukawa segment model. In this model one splits the rod charge into a number of N_s point charges along the rod. Each point charge interacts with the point charge of another neighbouring rod by a screened Coulomb potential as given in Equation (2) where now σ denotes the cylindrical diameter of the rods and the inverse Debye-Hückel screening length is

$$\kappa = \sqrt{\frac{4\pi e^2(Z\rho + 2n_s)}{\epsilon k_B T}}, \quad (4)$$

which is somewhat more general including additional screening from added salt ions, n_s denoting the concentration of monovalent added salt.

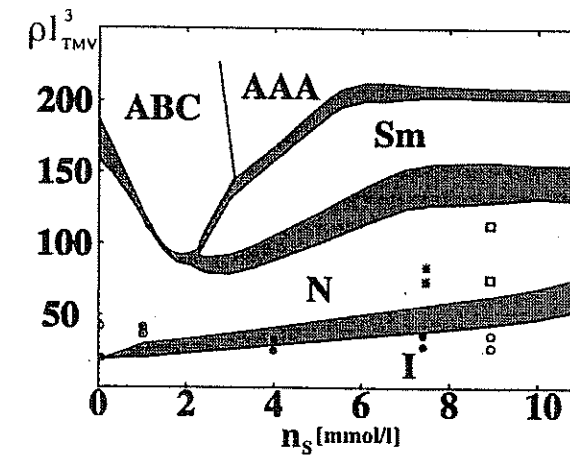


FIGURE 4: Phase diagram of the TMV: the coexistence densities in units of ℓ_{TMV}^{-3} are plotted versus the concentration n_s of added monovalent salt. The grey area marks the coexistence region. There is a stable isotropic phase (I), nematic phase (N), smectic A phase (Sm), and two different crystalline structures with an AAA and ABC stacking. From Ref. (43).

In order to predict the phase diagram theoretically, one needs the Helmholtz free energy in all possible phases. We anticipate here the occurrence of liquid-crystalline phases; as nematic, smectic and columnar phases. If the cell-model for the solid part is combined with scaled particle theory for the fluid part, one is able to construct a simple theory for hard spherocylinders (40, 41) which works remarkably well for the phase diagram if compared to computer simulations (42). The further idea is to split the full Yukawa-segment interaction into a short-ranged part which is mapped onto an effective

hard spherocylinder interaction and treat the rest in mean-field perturbation theory (43). The resulting phase diagram for TMV solution is shown in Fig. 4. We have taken a bare rod charge of $Z = 390$ and a number of $N_s = 17$ segments per rod. The phase diagram is plotted as a function of rod and added salt concentration. A variety of liquid crystalline phases is stable including nematic, smectic A and two fully crystalline phases with AAA and ABC stacking sequence. For fixed rod density, a nematic reentrant transition occurs upon increasing the concentration of added salt. The phase diagram compares qualitatively well with experimental data as discussed in detail in Ref. (43). It would be interesting to calculate the phase diagram by computer simulation in order to check whether the nematic reentrant transition is real or an artifact of the approximations.

CONCLUSIONS

In conclusion, colloidal suspensions are ideal model systems to study phase transformations. Since their effective interactions are tunable and their confinement is well-controlled, a wealth of novel phase transitions can be observed. It is remarkable that most of the progress in this field has been induced by a fruitful collaboration between experiment, computer simulations and experiment. Taking this for granted, we hope that the theoretical phase diagrams discussed in this paper can be verified (or disproved) in actual samples and that further interesting phases will be found which both enhance our fundamental understanding of mesoscopic matter and lead to new exciting applications.

ACKNOWLEDGEMENTS

We thank J. Wills for a helpful discussion and the Deutsche Forschungsgemeinschaft for financial support within the SFB 237 and the Gerhard-Hess-Programm.

REFERENCES

1. Baus, M., Rull, L. F., and Ryckaert, J. P. *Observation, Prediction and Simulation of Phase Transitions in Complex Fluids*, Series B: Physics, Dordrecht: Kluwer Academic Publishers, 1995.
2. Hafner, J., *From Hamiltonians to Phase Diagrams*, Springer Series in Solid-State Sciences, Berlin: Springer-Verlag, 1987.
3. Löwen, H., *Phys. Rep.* **237**, 249 (1994).
4. For a recent review, see Pusey, P. N., in *Liquids, Freezing and the Glass Transition*, Amsterdam: North Holland, 1991.

5. Hoover, W. G., Gray, S. G., Johnson, K. W., *J. Chem. Phys.* **55**, 1128 (1971); Robbins, M. O., Kremer, K., Grest, G. S., *J. Chem. Phys.* **88**, 3286 (1988).
6. Lutsko, J. F., Baus, M., *J. Phys. Condens. Matter* **3**, 6547 (1991).
7. McConnell, G. A., Gast, A. P., Huang, J. S., Smith, S. D., *Phys. Rev. Letters* **71**, 2102 (1993).
8. Sirota, E. B., Ou-Yang, H. D., Sinha, S. K., Chaikin, P. M., Axe, J. D., Fujii, Y., *Phys. Rev. Letters* **62**, 1524 (1989).
9. Ilett, S. M., Orrock, A., Poon, W. C.-K., Pusey, P. N., *Phys. Rev. E* **51**, 1344 (1995).
10. Bolhuis, P., Frenkel, D., *Phys. Rev. Letters* **72**, 2211 (1994).
11. Schmidt, M., Löwen, H., *Phys. Rev. Letters* **76**, 4552 (1996).
12. Schmidt, M., Löwen, H., *Phys. Rev. E* **55**, 7228 (1997).
13. Pansu, B., Pieranski, P., *J. Physique* **45**, 331 (1984).
14. Pieranski, P., Strzelecki, L., Pansu, B., *Phys. Rev. Letters* **50**, 900 (1983).
15. Van Winkle, D. H., Murray, C. A., *Phys. Rev. A* **34**, 562 (1986); Murray, C. A., Sprenger, W. O., Wenk, R. A., *Phys. Rev. B* **42**, 688 (1990); Murray, C. A., in: *Bond-orientational Order in Condensed Matter Systems*, New York: Springer, 1992.
16. Weiss, J., Oxtoby, D. W., Grier, D. G., Murray, C. A., *J. Chem. Phys.* **103**, 1180 (1995).
17. Nesper, S., Bechinger, C., Leiderer, P., Palberg, T., *Phys. Rev. Letters* **79**, 2348 (1997).
18. Rosenfeld, Y., Schmidt, M., Löwen, H., Tarazona, P., *J. Phys.: Condensed Matter* **8**, L577 (1996); *Phys. Rev. E* **55**, 4245 (1997).
19. Németh, Z. T., Löwen, H., *J. Phys.: Condensed Matter* **10**, 6189 (1998).
20. Bubeck, R., Nesper, S., Bechinger, C., Leiderer, P., *Prog. Colloid Polymer Science* **110**, 41 (1998); Zahn, K., Lenke, R., Maret, G., *Phys. Rev. Letters* **82**, 2721 (1999).
21. Peeters, F. M., in *Two Dimensional Electron Systems*, Amsterdam: Kluwer Academic Publishers, 1997, pp. 17-32; Peeters, F. M., Partoens, B., Schweigert, V. A., Goldoni, G., *Physica E* **1**, 219 (1997).
22. Mitchell, T. B., Bollinger, J. J., Dubin, E., Huang, X.-P., Itano, W. M., Baughman, R. H., *Science* **282**, 1290 (1998).
23. Molnár, J., *Acta Mathematica Academiae Scientiarum Hungaricae* **31**, 173 (1978).
24. See e.g.: Cipra, B., *Science* **281**, 1267 (1998).
25. Wills, J. M., *The Mathematical Intelligencer* **20**, 16 (1998).
26. For a review see: Grest, G. S., Fetters, L. J., Huang, J. S., Richter, D., *Advances in Chemical Physics*, Vol. XCIV, 67 (1996).
27. Witten, T. A., Pincus, P. A., *Macromolecules* **19**, 2509 (1986).

28. Likos, C. N., Löwen, H., Watzlawek, M., Abbas, B., Jucknischke, O., Allgaier, J., Richter, D. *Phys. Rev. Letters* **80**, 4450 (1998).
29. Jusufi, A., Watzlawek, M., Löwen, H., *Macromolecules* **32**, 4470 (1999).
30. Stellbrink, J., Abbas, B., Allgaier, J., Monkenbusch, M., Richter, D., Likos, C. N., Löwen, H., Watzlawek, M. *Prog. Colloid Interface Science* **110**, 25 (1998).
31. Watzlawek, M., Likos, C. N., Löwen, H., *Phys. Rev. Letters* **82**, 5289 (1999).
32. Witten, T. A., Pincus, P. A., Cates, M. E., *Europhys. Lett.* **2**, 137 (1986).
33. McConnell, G. A., Gast, A. P., *Macromolecules* **30**, 435 (1997).
34. von Ferber, C., Jusufi, A., Likos, C. N., Löwen, H., Watzlawek, M., to be published.
35. Likos, C. N., Löwen, H., Poppe, A., Willner, L., Roovers, J., Cubitt, B., Richter, D., *Phys. Rev. E* **58**, 6299 (1998).
36. Likos, C. N., Vaynberg, K. A., Löwen, H., Wagner, N. J., to be published in *Langmuir*.
37. Asakura, S., Oosawa, F., *J. Chem. Phys.* **22**, 1255 (1954).
38. Denton, A. R., Löwen, H., *Phys. Rev. Letters* **81**, 469 (1998).
39. Löwen, H., *Phys. Rev. Letters* **72**, 424 (1994); *J. Chem. Phys.* **100**, 6738 (1994).
40. Graf, H., Löwen, H., Schmidt, M., *Prog. Colloid Polymer Science* **104**, 177 (1997).
41. Graf, H., Löwen, H., *J. Phys.: (Condensed Matter)* **11**, 1435 (1999).
42. Bolhuis, P., Frenkel, D., *J. Chem. Phys.* **106**, 666 (1997).
43. Graf, H., Löwen, H., *Phys. Rev. E* **59**, 1932 (1999).